Iron(II) Complexes of the Linear *rac*-tetraphos-1 Ligand as Efficient Homogeneous Catalysts for Sodium Bicarbonate Hydrogenation and Formic Acid Dehydrogenation.

Federica Bertini, Irene Mellone, Andrea Ienco, Maurizio Peruzzini, and Luca Gonsalvi.*

Consiglio Nazionale delle Ricerche, Istituto di Chimica dei Composti Organometallici (CNR-ICCOM), Via Madonna del Piano 10, 50019 Sesto Fiorentino (Firenze), Italy.

KEYWORDS: iron phosphine complexes; formic acid dehydrogenation; bicarbonate hydrogenation; X-ray crystallography; HPNMR mechanistic studies

ABSTRACT: The linear tetraphosphine 1,1,4,7,10,10-hexaphenyl-1,4,7,10-tetraphosphadecane (tetraphos-1, P4) was used as *rac*- and *meso*-isomers for the synthesis of both molecularly defined and *in situ* formed Fe(II) complexes. These were used as precatalysts for sodium bicarbonate hydrogenation to formate and formic acid dehydrogenation to hydrogen and carbon dioxide with good activities under mild conditions. Mechanistic details of the reaction pathways were obtained by NMR and HPNMR experiments highlighting the role of the Fe(II) monohydrido complex $[FeH(\textit{rac}\text{-P4})]^+$ as key intermediate. X-ray crystal structures of different complexes bearing *rac*-P4 were also obtained and are here described.

INTRODUCTION

Hydrogen is of crucial importance in the chemical industry and holds great potential as secondary energy carrier, as feedstock for direct hydrogen fuel cells.[1] Its generation from renewable sources and its storage in a safe and reversible manner are urgent targets for a widespread application of hydrogen in such technologies. Among the different H_2 storage materials, formic acid (FA) is a non-toxic hydrogen source which can be handled and transported easily, and possesses a relatively high H_2 content (4.4 wt %). H_2 generation from formic acid affords H_2 + CO_2 mixtures and is therefore an "atom efficient" process, since no hydrogen is wasted in the formation of by-products (such as H_2O, as in the case of H_2 generation from methanol or methane). In addition, the by-product CO_2 can be, in the presence of suitable catalysts, re-hydrogenated back to FA, affording a zero-carbon footprint cycle for hydrogen storage and release.[2] The efficient interconversion of FA to H_2 and CO_2 is of importance for both H_2 storage and release, and for the utilization of CO_2 or bicarbonates obtained by its trapping in alkaline water solutions, as a abundant C1-feedstock. In the past decade, there have been a number of reports on selective FA dehydrogenation to produce CO-free H_2, as well as on the hydrogenation of CO_2 or bicarbonates to FA or formate salts. However, most of these catalysts are based on low-abundant noble metals such as ruthenium[3] or iridium[4]. Only recently, this chemistry has been extended to non-noble metals such as Fe[5] and Co.[6]

The most active additive-free Fe-based catalyst system for FA dehydrogenation under mild temperature conditions (40 °C) reported to date was obtained by combining the iron(II) salt $Fe(BF_4)_2{\cdot}6H_2O$ with the tetraphosphine ligand $P(CH_2CH_2PPh_2)_3$ (PP_3).[5e,7] Although the nature of the initial complex formed in this reaction has not been fully ascertained, mechanistic studies indicated that under catalytic conditions (FA in propylene carbonate, PC) complexes $[FeH(PP_3)]^+$ and $[FeH(\eta^2\text{-}H_2)(PP_3)]^+$ are formed.[5e,8] This catalytic system was successfully applied to bicarbonates hydrogenation to formates and carbon dioxide valorization to alkyl formates and formamides.[5a] In continuation of this work, efficient iron-catalyzed hydrogenation of carbon dioxide and bicarbonates was achieved using $Fe(BF_4)_2{\cdot}6H_2O$ and $P^{Ph}P_3$ [$P^{Ph}P_3$ = tris(2-(diphenylphosphino)phenylphosphine]. In this case, metal complexation afforded the well defined complex $[FeF(P^{Ph}P_3)]^+$ *via* F–BF_3 activation. Mechanistic studies established that this complex reacts with H_2 to give $[FeH(\eta^2\text{-}H_2)(P^{Ph}P_3)]^+$. High pressure HPNMR CO_2 hydrogenation experiments in the presence of NEt_3 suggested the formation of the known dihydride complex $[Fe(H)_2(P^{Ph}P_3)]$.[5f]

In recent years, our group has been interested in FA dehydrogenation and CO_2 hydrogenation, so far using Ru[9] and Ir[10] homogeneous catalysts. In an effort to develop novel, non-noble metal-based catalysts for such transformations, we became eager to explore the potential of Fe(II) complexes of other tetradentate phosphines.

The linear tetradentate phosphine ligand 1,1,4,7,10,10-hexaphenyl-1,4,7,10-tetraphosphadecane (tetraphos-1, P4) exists as a mixture of *racemic* (S,S,R,R) and *meso* (S,R) diastereoisomers (hereafter *rac*-P4 and *meso*-P4, respectively), which can be separated by fractional crystallization.[11,12] Despite the existence of these stereoisomers was recognized as early as in 1974,[13] the importance of this isomerism was not fully appreciated until the work of Brown and Canning.[11] The configurations that these diastereoisomers can adopt in an octahedral complex are denoted as *cis*-α, *cis*-β and *trans* (Chart 1). While the *meso* isomer can adopt only a *trans* or *cis*-β configuration, all three configurations are physically possible for the *rac* isomer. Nevertheless, the *rac* isomer is known for its propensity to form *cis*-α complexes.[11,14] Since the original preparation of tetraphos-1 by King and co-workers,[15] there have been a number of reports on its coordination behavior.[11-16] By a close perusal of available literature, we noticed that the chemistry of the *meso* isomer is

far more developed than that of the *rac* isomer. Only complexes [FeBr(P4)][BPh_4][16d] and *trans*-[FeH(N_2)(P4)][16c] were characterized crystallographically and in both the ligand exhibits a *meso* configuration. This was probably due to the fact that the authors used commercial tetraphos-1 which is richer in the *meso* isomer. The syntheses of [FeH(P4)]X, [Fe(NCS)$_2$(P4)], [FeH(NCS)(P4)]X, and [FeH(CO)(P4)] (X = Br, I) were also described, but no indications on the configuration of the P4 ligand was provided.[16e] Morris and co-workers reported on the hydrogen exchange between η^2-H_2 and hydride ligands in *trans*-[FeH(η^2-H_2)(*meso*-P4)]BF_4, obtained by protonation of the corresponding dihydride complex *trans*-[Fe(H)$_2$(*meso*-P4)].[12,14] To the best of our knowledge, the full exploration of the coordination chemistry of *rac*-P4 to Fe(II) and the reactivity of the complexes so obtained has never been reported.

In this work, we describe the synthesis of novel Fe(II) complexes bearing *rac*-P4, their reactivity toward H_2 and CO_2, and their application as efficient catalysts for FA dehydrogenation and sodium bicarbonate hydrogenation to sodium formate. The catalytic data are complemented by mechanistic details obtained by model stoichiometric reactions and *in operando* high pressure HPNMR experiments.

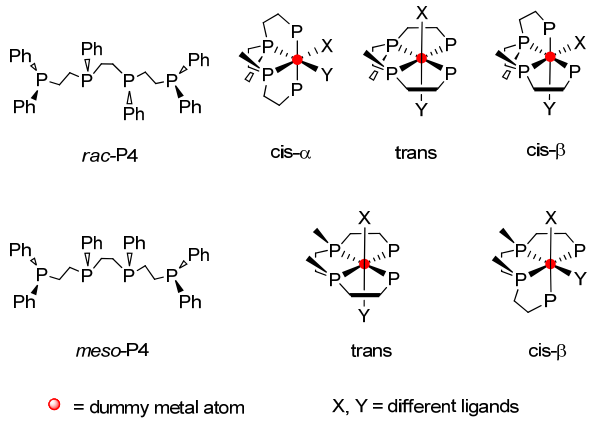

Chart 1. The *rac* and *meso* isomers of tetraphos-1 (P4) and allowed configurations for their octahedral complexes.

RESULTS AND DISCUSSION

Syntheses and characterization of Fe(II) complexes. At first, *rac*-P4 and *meso*-P4 were obtained in pure isomeric form from the commercial ligand P4, containing a *rac:meso* = 1:3 ratio, by fractional crystallization as described in the literature.[14] In order to test the coordination abilities of the two isomers with suitable iron(II) sources, the commercially available salt $Fe(BF_4)_2{\cdot}6H_2O$ and the easily accessible complex[17] $[Fe(CH_3CN)_6](BF_4)_2$ were used as metal precursors. The reaction of $Fe(BF_4)_2{\cdot}6H_2O$ with *rac*-P4 (1:1) resulted rather sluggish in a variety of common solvents, whereas it proceeded smoothly in propylene carbonate (PC), affording a deep purple solution. The $^{31}P\{^1H\}$ NMR spectrum of such solution (C_6D_6 insert) showed two broad signals at δ_P 99.9 and 60.9 ppm, indicative of Fe(II) complexation by the ligand. $^{19}F\{^1H\}$ NMR analysis at room temperature showed only a single, sharp peak for the BF_4 anion, suggesting that B–F activation to form the putative fluoride complex [FeF(*rac*-P4)](BF_4), in a similar way to what observed by Beller *et al.*[5f] for $[FeF(P^{Ph}P_3)]^+$ had not occurred. We could also exclude the formation of a complex bearing PC as ancillary ligand, since the same $^{31}P\{^1H\}$ NMR pattern was observed in the absence of PC (for example, in CD_2Cl_2). Due to the known propensity of Fe(P4) complexes to adopt a pentacoordinate geometry, often completed by halide ligands,[16c,d,f] we propose that under these conditions the highly reactive complex [Fe(η^1-FBF_3)(*rac*-P4)](BF_4) (**1**) has formed, where one of the BF_4 counterions acts as a weakly coordinating ligand (Scheme 1).[18] Upon addition of CD_3OD to a solution of **1** in PC, a new species is formed, and the corresponding $^{31}P\{^1H\}$ NMR pattern gives two triplets at δ_P 107.6 and 73.8 ($^2J_{PP}$ = 29.9 Hz). This behavior may be attributed to the displacement of the loosely coordinated BF_4 anion by methanol, yielding a solvento-species such as [Fe(CD_3OD)$_x$(*rac*-P4)](BF_4)$_2$ (**1'**, x = 1 or 2). To date, all our attempts to obtain crystals of either **1** or **1'** failed. A similar reactivity was observed upon reacting $Fe(BF_4)_2{\cdot}6H_2O$ with *meso*–P4, which resulted in the formation of a brown solution containing the putative complex [Fe(η^1-FBF_3)(*meso*-P4)](BF_4) (**1"**) also characterized by two broad signals in the $^{31}P\{^1H\}$ NMR at δ_P 104.8 and 70.8 ppm.

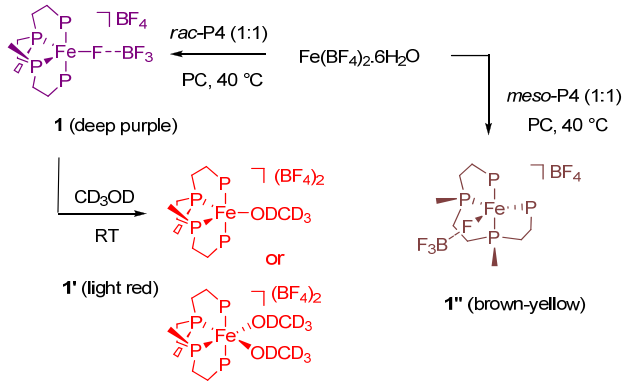

Scheme 1. Reactivity of $Fe(BF_4)_2{\cdot}6H_2O$ with *rac*-P4 and *meso*-P4 to give **1, 1'** and **1"**.

In contrast, the reaction of *rac*-P4 with $[Fe(CH_3CN)_6](BF_4)_2$ resulted in the quantitative formation of the well-defined complex *cis*-α-[Fe(CH_3CN)$_2$(*rac*-P4)](BF_4)$_2$ (**2**) as the sole product (Scheme 2). The $^{31}P\{^1H\}$ NMR spectrum exhibits two triplets at 100.7 and 65.6 ppm in CD_3CN, which reflect an AA'XX' coupling pattern with equivalent *cis*-P,P coupling constants ($^2J_{PP}$ = 31.7 Hz). These values are in close analogy with those attributed by Habeck *et al.* to *cis*-α-[Fe(NCS)$_2$(*rac*-^{pr}P4)] (*rac*-^{pr}P4 = 1,1,4,8,11,11-hexaphenyl-1,4,8,11-tetraphosphaundecane].[19] Crystals suitable for X-ray diffraction analysis were grown by adding *n*-pentane to a solution of **2** in acetonitrile/methanol (Figure 1). Complex **2** crystallizes in the C2/c space group and has an octahedral coordination geometry at the Fe(II) center, with the Fe–P_{ax} distances (Fe1–P1 = 2.2868(13) Å and Fe1–P4 = 2.2982(13) Å) that are longer than the Fe–P_{eq} distances (Fe1–P2 2.2138(13) and Fe1–P3 2.2247(12) Å). Notably, complex **2** resulted air stable as a solid and solutions in acetonitrile/methanol could be stored under nitrogen for over a month without any appreciable decomposition. In contrast, reaction of *meso*-P4 with $[Fe(CH_3CN)_6](BF_4)_2$ was not selective, and afforded a mixture of two products in approximately 2:1 ratio, which were identified on the basis of characteristic

$^{31}P\{^{1}H\}$ NMR resonances[12,19] (see Supporting Information), as the *trans*- and *cis*-β isomers of $[Fe(CH_3CN)_2(meso\text{-}P4)](BF_4)_2$, respectively.

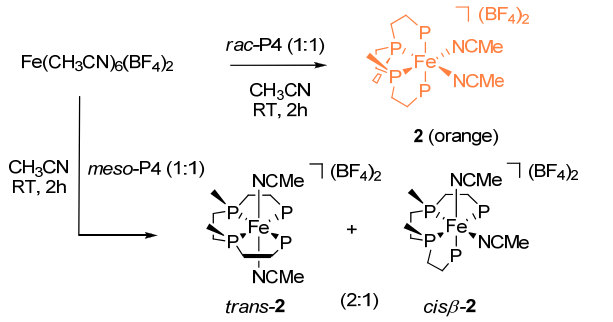

Scheme 2. Synthesis of *rac*-P4 and *meso*-P4 complexes starting from $[Fe(CH_3CN)_6](BF_4)_2$.

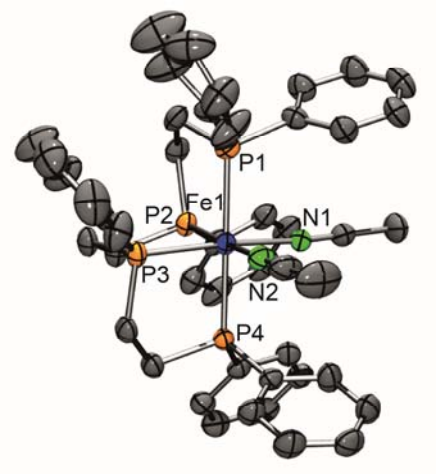

Figure 1. Molecular structure for the cationic portion of **2**. Ellipsoids are set at 50% probability. Hydrogen atoms are omitted for clarity. Selected bond lengths (Å) and bond angles (°): Fe1–N1 1.943(3); Fe1–N2 1.955(4); Fe1–P1 2.2868(13); Fe1–P2 2.2138(12); Fe1–P3 2.2247(12); Fe1–P4 2.2982(13). N1–Fe1–N2 88.70(15); N2–Fe1–P3 93.76(11); P2–Fe1–P3 85.26(4); P2–Fe1–N1 92.51(11); P1–Fe1–N1 90.36(11); P1–Fe1–N2 91.58(12); P1–Fe1–P2 85.87(5); P1–Fe1–P3 94.48(5); P1–Fe1–P4 179.53(5); P2–Fe1–P4 94.29(5); P3–Fe1–P4 85.10(4).

Syntheses of Fe(*rac*-P4) hydrido-complexes. Due to the relevance of Fe-hydrido complexes to FA dehydrogenation and bicarbonate hydrogenation reactions, we targeted the syntheses of the so far unknown mono- and dihydride iron complexes of *rac*-P4. The analogues of the *meso* isomer have been previously reported.[12,16e] The monohydrido complex $[FeH(rac\text{-}P4)][BPh_4]$ (**3**·BPh_4) was obtained upon reacting *rac*-P4, anhydrous $FeCl_2$, $NaBPh_4$ and $NaBH_4$ in stoichiometric amounts in THF/MeOH, and was characterized by NMR and X-ray diffraction studies upon growing suitable crystals from these solutions. The $^{31}P\{^{1}H\}$ NMR spectrum of **3**·BPh_4 in d_8-THF showed two triplets at δ_P 119.4 and 99.4 ppm, reflecting an AA'XX' coupling pattern with an observed splitting of 24.5 Hz, while in the corresponding ^{1}H NMR spectrum, the hydride signal appears as a broad triplet at -9.16 ppm ($^{2}J_{HP}$ = 24.0 Hz). The crystal structure of **3**·BPh_4 displays a pseudo-octahedral geometry, with the hydride ligand occupying alternatively one or the other *cis* positions in 50% occupancy (Figure 2). The distortion from the ideal octahedral geometry is evident from the P1–Fe1–P4 angle (170.4°), which is significantly bent compared to the analogous P1–Fe1–P4 angle in **2** (179.5°), whereas the P2–Fe1–P3 angle is comparable in **2** and **3** (85.3° vs. 85.7°).

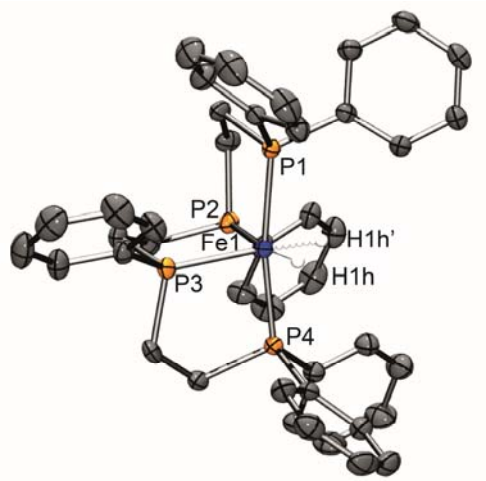

Figure 2. Molecular structure for the cationic portion of **3**·BPh_4. Ellipsoids are set at 50% probability. Hydrogen atoms are omitted for clarity except the hydrido ligand**.** Selected bond lengths (Å) and bond angles (°): Fe1–P1 2.2189(7); Fe1–P2 2.1961(7); Fe1–P3 2.2207(7); Fe1–P4 2.1993(8); Fe1–H1h 1.61(5); Fe1–H1h' 1.41(5); H1h–Fe1–H1h' 90(3); P1–Fe1–P2 85.38(3); P1–Fe1–P3 102.58(3); P1–Fe1–P4 170.41(3); P2–Fe1–P3 85.74(3); P2–Fe1–P4 96.87(3); P3–Fe1–P4 86.91(3); H1h–Fe1–P1 89.0(2); H1h–Fe1–P2 172.4(18); H1h–Fe1–P3 100.6(18); H1h–Fe1–P4 87.(2); H1h'–Fe1–P1 83.(2); H1h'–Fe1–P2 83.(2); H1h'–Fe1–P3 168(2); H1h'–Fe1–P4 87 (2).

The neutral dihydrido complex *cis*-α-$[Fe(H)_2(rac\text{-}P4)]$ (**4**) was synthesised from *rac*-P4, anhydrous $FeCl_2$ and excess $NaBH_4$ under reflux conditions in a THF/EtOH mixture. The $^{31}P\{^{1}H\}$ NMR spectrum of **4** in d_8-THF displayed two triplets at δ_P 123.8 and 113.1 ppm with a $^{2}J_{PP}$ = 13.5 Hz due to *cis*-P_2P coupling, whereas the two hydride ligands gave a complex multiplet centered at -11.7 ppm (apparent double septuplet; see SI). Crystals of **4** suitable for X-ray analysis were grown by diffusion of MeOH into the solution which resulted from the reaction mixture, after filtration and partial evaporation of the solvent. The solid state molecular structure of **4** displays a significantly distorted octahedral coordination geometry at the Fe(II) center with the *rac*-P4 ligand adopting a *cis*-α configuration (Figure 3). The P1–Fe1–P4 angle in **4** (159.6°) is significantly more distorted than in **3**·BPh_4 (170.4°). Furthermore, all Fe–P bond distances are significantly shorter (all < 2.17 Å) respect to those observed in **2** (2.19 – 2.22 Å) and **3**·BPh_4 (2.21 – 2.30 Å).

Reactivity of 1 and 2 toward H_2. To verify the potential of **1** and **2** as hydrogenation catalyst precursors, we investigated at first their reactivity towards molecular H_2 in model reactions. Bubbling H_2 (1 atm) into a solution of **1** in PC at room temperature resulted in the quantitative formation of the monohydrido complex **3**·BF_4, having identical NMR patterns as the isolated **3**·BPh_4. Notably, the heterolytic H–H cleavage promoted by the Fe/P4 system **1** occurs *without* an additional base.[20]

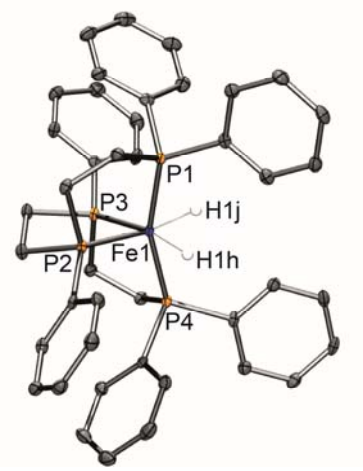

Figure 3. Molecular structure of **4**. Ellipsoids are set at 50% probability. Hydrogen atoms are omitted for clarity except hydrido ligands. Selected bond lengths (Å) and bond angles (°): Fe1–P1 2.1249(7); Fe1–P2 2.1510(7); Fe1–P3 2.1654(7); Fe1–P4 2.1303(7); Fe1–H1h 1.55(3); Fe1–H1j 1.57(2); H1h–Fe1–H1j 90.6(13); P1–Fe1–P2 89.00(3); P1–Fe1–P3 106.14(3); P1–Fe1–P4 159.62(3); P2–Fe1–P3 86.05(2); P2–Fe1–P4 106.21(3); P3–Fe1–P4 88.71(3); H1h–Fe1–P1 85.0(9); H1h–Fe1–P2 91.8(9); H1h–Fe1–P3 168.6(9); H1h–Fe1–P4 81.1(9); H1j–Fe1–P1 82.3(9); H1j–Fe1–P2 93.3(9); H1j–Fe1–P3 171.8(9); H1j–Fe1–P4 83.0(9).

The experiment was repeated under a pressure of H_2 (30 bar) and monitored by high pressure HPNMR spectroscopy. A solution of $Fe(BF_4)_2{\cdot}6H_2O$ and *rac*-P4 in PC (1.5 mL, 0.01M) was initially transferred in a 10 mm medium-pressure HPNMR sapphire tube. $^{31}P\{^1H\}$ NMR analysis at room temperature under Ar atmosphere showed, as expected, the broad signals due to **1**. Upon addition of CD_3OD for deuterium lock (0.5 mL), the $^{31}P\{^1H\}$ NMR pattern due to **1'** appeared, while no hydride signals were observed in the corresponding ^1H NMR spectrum. The tube was then pressurized at RT with 40 bar H_2, which resulted in the quantitative conversion of **1** and **1'** into the monohydride **3**·BF_4. In a variable temperature (VT) NMR experiment in the temperature range 233–353 K we never observed the formation of a hydrido-dihydrogen complex such as $[FeH(\eta^2\text{-}H_2)(rac\text{-P4})]^+$, in analogy to what previously described for $[FeH(meso\text{-P4})]^+$.[14]

Complex **2** resulted remarkably less reactive towards H_2 than **1**. Bubbling H_2 (1 atm) into a solution of **2** in CD_3OD did not result in any visible changes in the initial $^{31}P\{^1H\}$ NMR pattern. Under 30 bar H_2 pressure (HPNMR experiment, see SI), besides the peaks of unreacted **2**, four distinct $^{31}P\{^1H\}$ NMR resonances were observed, having equal intensities, at δ_P 121.7 (br.s), 104.0 (br.d), 101.2 (br.d), 96.3 (br.s). The corresponding ^1H NMR spectrum showed a complex signal centered at δ_H -8.5 ppm (dq, $^2J_{HPtrans}$ 36.7 Hz, $^2J_{HPcis,eq}$ Hz, 51.3 $^2J_{HPcis,ax1} = {}^2J_{HPcis,ax2}$ = 51.1 MHz). These patterns, indicative of unequivalent phosphorus atoms typical of an octahedral Fe complex, were attributed to the formation of *cis-α*-[FeH(NCMe)(*rac*-P4)](BF_4) (**5**). Upon heating to 40 °C, we observed also the formation of **3**·BF_4 (see SI for details). However, quantitative transformation of **2** could be achieved only in the presence of an added base (NEt_3), affording at first a mixture of **3**·BF_4 and **5** (upon heating), and then **5** as the final product. Addition of Et_2O/pentane to the reaction mixture resulted in the precipitation of yellow crystals of **5**. The corresponding (highly disorderd) X-ray crystal structure confirmed the proposed formula (see SI). This behavior is likely due to the lower reactivity of **2** with H_2 due to the better donor properties to Fe of the MeCN ligands compared to the loosely bound η^1-FBF_3 in **1**. As a consequence, MeCN elimination in passing from **2** to **3**·BF_4 follows a stepwise pathway involving the stable intermediate **5** (Scheme 3). A different Lewis acidity of the Fe center in these complexes must also be involved.[20]

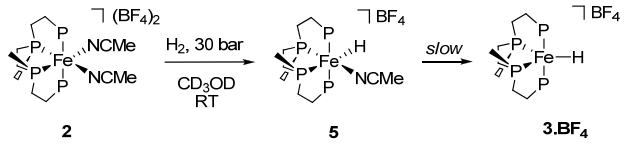

Scheme 3. Conversion of **2** to **3**·BF_4 *via* intermediate **5**.

Reactivity of 3·BPh_4 and 4 toward CO_2. In the next step, we explored the reactivity of the mono- and dihydrides **3**·BPh_4 and **4** toward CO_2. Beller *et al.* showed that insertion of CO_2 into the Fe–H bond of complex $[FeH(PP_3)]^+$ could be achieved under 10 atm of gas pressure giving the corresponding formate complex.5[a] In an NMR-scale experiment, we reacted the monohydride **3**·BPh_4 with CO_2 (1 atm) in d_8-THF, obtaining as expected, the formate complex *cis-α*-[Fe(η^2-O_2CH)(*rac*-P4)](BPh_4) (**6**·BPh_4, Scheme 4), having $^{31}P\{^1H\}$ NMR signals at δ_P 106.8 (t) and 77.4 (t, $^2J_{PP}$ = 29.5 Hz). In the corresponding $^{13}C\{^1H\}$ NMR spectrum, apart from the signal at δ_C 162.4 ppm due to BPh_4^-, a broad singlet at 171.9 ppm, compatible with a coordinated formate anion, was observed.[5a,21] Unfortunately, the ^1H NMR expected in the range 8.2-8.5 ppm for the formate ligand, diagnostic for η^1 vs. η^2-coordination, was lying under the ligand aromatic protons multiplet. After 24 h, the $^{31}P\{^1H\}$ NMR spectrum showed signals of a new complex with triplets at δ_P 107.5 and 74.1 ppm ($^2J_{PP}$ = 30.4 Hz), which we assigned to the neutral carbonate complex *cisα*-[Fe(η^2-O_2CO)(*rac*-P4)] (**7**). The attribution was confirmed by independent synthesis of **7** by reaction of **1** with an excess of K_2CO_3 in PC. In addition, the formation of complex **7** was observed also in HPNMR experiments upon reacting either **1** or **2** with $NaHCO_3$ (*vide infra*).

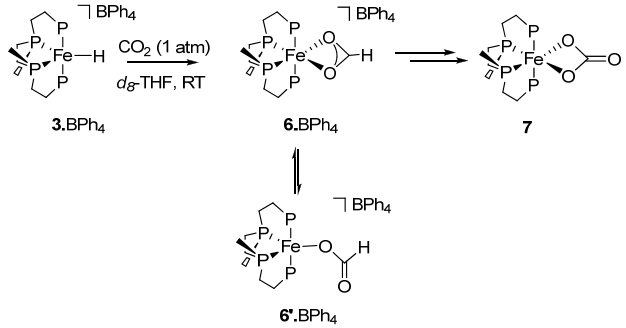

Scheme 4. Reactivity of complex **3**·BPh_4 with H_2 to give **6**·BPh_4 and **7**.

MeOH diffusion into the d_8-THF solution recovered after the NMR experiment described above afforded few purple crystals which were found to be suitable for X-ray diffraction data collection. Quite surprisingly, the solid-state structure revealed a trimetallic unit in which a central $[Fe(MeOH)_4]^{2+}$ moiety, bridges two [Fe(O_2CO)(*rac*-P4)] moieties via the two carbonate ligands by η^1-O coordination, as shown in Figure 4. Despite the

fact that the formation of complex {μ^2-[Fe(MeOH)$_4$]-κ^1-*O*-[Fe(η^2-O$_2$CO)(*rac*-P4)]$_2$}(BPh$_4$)$_2$ (**7'**) may be accidental, its solid-state structure confirmed the presence of CO_3^{2-} ligands. Carbonate is likely to form by reductive disproportionation of CO_2 into CO_3^{2-} and CO, promoted by **3**·BPh$_4$.[22] This reaction, occurring via a formate intermediate, has been previously described with Fe(II) hydrido-complexes such as *trans*-[Fe(H)$_2$(dppe)$_2$] and [Fe(H)$_2$(PP$_3$)].[22,23]

Complex **4** was also tested for reactivity with CO_2, to check for the possible formation of Fe-hydrido formate complexes, similarly to what proposed by Beller *et al.* for [Fe(H)$_2$(P^{Ph}P$_3$)].[5f] No reaction was observed under the conditions described above (*i.e.* 1 atm CO_2 in d_8-THF, RT). The experiment was repeated under moderate pressure of CO_2 (7 bar) under HPNMR conditions, but again no reaction occurred.

Fe-Catalyzed Sodium Bicarbonate Hydrogenation. The added base-free hydrogenation of sodium bicarbonate to formate in MeOH was tested in stainless steel autoclaves at different H_2 pressures and temperatures. In a preliminary experiment, we tested the activity of a combination of commercial tetraphos-1 (P4) and Fe(BF$_4$)$_2$·6H$_2$O (0.01 mmol, 1:1 ratio) in the hydrogenation of sodium bicarbonate in MeOH. To our delight, at 80 °C under 30 bar H_2, sodium formate was formed with TON = 154 (entry 1). The activity of **1** and **1"** was then tested to check for ligand effects.

The *in situ* formed pre-catalysts were obtained from stock solutions made from Fe(BF$_4$)$_2$·6H$_2$O and either *rac*-P4 or *meso*-P4 (0.01M in PC). The solutions were analyzed by $^{31}P\{^1H\}$ NMR before use to confirm the formation of the corresponding Fe(II) complexes **1** and **1"**. Catalyst precursor **1"** gave a rather poor catalytic performance, reaching a TON = 62 after 24 h under 60 bar H_2 and 80 °C using 0.1%mol catalyst (Table 1; entry 2). In contrast, **1** resulted rather active in the catalytic hydrogenation of $NaHCO_3$ in MeOH. Under 60 bar H_2 pressure, using 0.1 %mol catalyst, rather good yields (58% and 59%) and TONs (575 and 588) were achieved at 80 °C and 100 °C, respectively (Table 1; entries 3 and 4). TON values are in the order of magnitude obtained by Beller *et al.* with the Fe(BF$_4$)$_2$/PP$_3$ system under comparable conditions.[5a] At 60 °C (entry 5) the TON decreased to 186 with a formate yield of 19%. The effect of H_2 pressure on the productivity of the reaction was also tested. TON and yield were not affected at 80 °C in passing from 60 to 30 bar (entry 6), whereas at 10 bar the yield of formate was slightly reduced (entry 7). Using a catalyst/substrate ratio = 1:10000, significantly lower TON and yield were obtained (entry 8). At an intermediate catalyst/substrate ratio (1:3000, obtained by increasing the substrate concentration) good activity was observed with TON = 723 and 24% yield in formate (entry 9). The hydrogenation of $NaHCO_3$ to $NaHCO_2$ using the well-defined molecular complex **2** as catalyst precursor (0.1 mol%) proceeded smoothly at 80 °C, affording sodium formate in excellent yields (76 and 71%) and good TONs (762 and 766) under 60 and 30 bar H_2 pressure (entries 10 and 13, respectively). Lowering the catalyst loading to 0.01 mol%, an increased TON = 1229 was measured, albeit with a lower yield in formate (12%) (entry 14). At this catalyst/substrate ratio, **2** performed better than **1** (1.2 mmol sodium formate vs. ca. 0.1 mmol obtained, entries 14 and 8, respectively). Finally, at higher (100 °C) or lower temperatures (60 °C) in the presence of **2** (0.1 mol%), lower yields of formate were obtained (entries 11 and 12).

Mechanistic studies. To gain mechanistic insights into the iron-catalysed hydrogenation of $NaHCO_3$ to sodium formate in the presence of the best performing catalysts tested, namely **1** and **2**, we monitored the catalyst evolution by HPNMR spectroscopy under *in operando* conditions. In details, a 10 mm HPNMR sapphire tube was initially charged with a 0.01M solution of **1** in PC (1.5 mL), CD_3OD (0.5 mL) and $NaHCO_3$ (84 mg; 1.0 mmol, 100 equiv). The $^{31}P\{^1H\}$ NMR pattern showed the presence of **1** (25%), **1'**(25%) and of the carbonate complex **7** (50%) (percentages are based on integrals). Pressurization of the reaction mixture with H_2 (30 bar) resulted in the formation of the monohydride complex **3**·BF$_4$ (34%) at room temperature. The mixture composition evolved fully to **3**·BF$_4$ in less than 2h upon slow heating to 60 ºC, as confirmed by $^{31}P\{^1H\}$ NMR spectra. Further heating to 80 ºC did not result in further changes of the NMR patterns. The relative rate of conversion of complexes **1**, **1'** and **7** into **3**·BF$_4$ follows the order **1** >> **1'** > **7**.

A similar experiment was carried out using **2** (0.01 mmol) and $NaHCO_3$ (100 equiv) in CD_3OD (2 mL). The initial mixture prepared under Ar atmosphere showed in the corresponding $^{31}P\{^1H\}$ NMR the presence of unreacted **2** (84%), **7** (7%), and a new minor species **8** (9%), characterized by two triplets at δ_P 105.4 and 68.7 ppm ($^2J_{PP}$ = 30 Hz).[24] Upon standing at room temperature for 75 min, the resonances observed for **7** and **8** increased significantly (up to 34% and 27%), by slow reaction of **2** with $NaHCO_3$. The slow ligand exchange from CH_3CN to CO_3^{2-} mirrors the reactivity of **2** with H_2 described above. By pressurization of the HPNMR tube with H_2 (30 bar), the resonances due to **5** appeared in the $^{31}P\{^1H\}$ and ^1H NMR spectra, already at room temperature. At 80 °C, the signals of **2**, **7** and **8** disappeared, with concomitant formation of **3**·BF$_4$ and **5** and free sodium formate (broad signals at 8.6-8.9 in the ^1H NMR spectrum). The experimental results clearly indicate in **3**·BF$_4$ the key intermediate in the catalytic hydrogenation of $NaHCO_3$ with **1** and **2**, similarly to what described by Beller and co-workers in the case of CO_2 hydrogenation by [Fe(H)(PP$_3$)]$^+$.[5a] A proposed mechanism accounting for the observed reactivity is shown in Scheme 5.

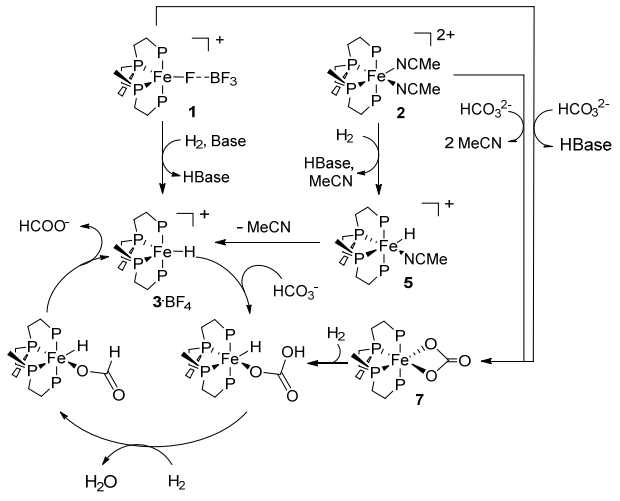

Scheme 5. Proposed mechanism for the catalytic hydrogenation of $NaHCO_3$ in the presence of **1** and **2**.

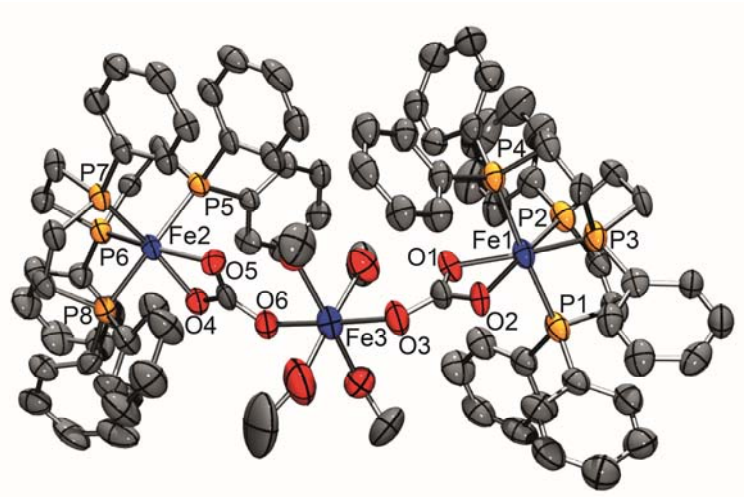

Figure 4. Molecular structure for the cationic part of {μ^2-[Fe(MeOH)$_4$]-κ^1-*O*-[Fe(η^2-O$_2$CO)(*rac*-P4)]$_2$}(BPh$_4$)$_2$ (**7'**). Ellipsoids are set at 50% probability. Hydrogen atoms are omitted for clarity. Selected bond lengths (Å) and bond angles (°): Fe(1)–O(1) 2.034(5); Fe(1)–O(2) 2.029(5); Fe(1)–P(1) 2.287(3); Fe(1)–P(2) 2.204(3); Fe(1)–P(3) 2.198(2); Fe(1)–P(4) 2.296(3); Fe(2)–O(4) 2.032(5); Fe(2)–O(5) 2.045(5); Fe(2)-P(5) 2.282(2); Fe(2)–P(6) 2.217(3); Fe(2)–P(7) 2.203(2); Fe(2)–P(8) 2.260(2); Fe(3)–O(3) 2.133(6); Fe(3)–O(6) 2.077(6); O(2)–Fe(1)–O(1) 65.0(2); O(2)–Fe(1)–P(3) 104.37(18); O(1)–Fe(1) –P(3) 165.38(18); O(2)–Fe(1)–P(2) 167.62(17); O(1)–Fe(1)–P(2) 106.28(19); P(3)–Fe(1)–P(2) 85.68(9); O(2)–Fe(1)–P(1) 87.62(17); O(1)–Fe(1)–P(1) 96.23(17); P(3)–Fe(1)–P(1) 93.20(9); P(2)–Fe(1)–P(1) 84.57(9); O(2)–Fe(1)–P(4) 94.17(17); O(1)–Fe(1)–P(4) 86.72(17); P(3)–Fe(1)–P(4) 84.02(9); P(2)–Fe(1)–P(4) 94.06(10); P(1)–Fe(1)–P(4) 176.99(9); O(4)–Fe(2)–O(5) 64.8(2); O(4)–Fe(2)–P(7) 166.91(18); O(5)–Fe(2)–P(7) 107.33(16); O(4)–Fe(2)–P(6) 104.68(17); O(5)–Fe(2)–P(6) 164.85(16); P(7)–Fe(2)–P(6) 84.94(9); O(4)–Fe(2)–P(8) 86.44(16); O(5)–Fe(2)–P(8) 92.75(17); P(7)–Fe(2)–P(8) 83.46(9); P(6)–Fe(2)–P(8) 97.55(9); O(4)–Fe(2)–P(5) 93.82(16); O(5)–Fe(2)–P(5) 85.33(16); P(7)–Fe(2)–P(5) 95.95(9); P(6)–Fe(2)–P(5) 84.56(9); P(8)–Fe(2)–P(5) 177.73(10).

Table 1. Hydrogenation of sodium bicarbonate using either *in situ* formed or defined molecular Fe(II) pre-catalysts.[a]

Entry	Catalyst precursor	substrate /catalyst	T (°C)	p (H$_2$) (bar)	TON[i,k]	Yield (%)[j,k]
1[b]	**i**	1000	80	60	154(±4)	15(±0)
2[c]	**1"**	1000	80	60	62(±16)	6(±2)
3[d]	**1**	1000	80	60	575(±52)	58(±5)
4[d]	**1**	1000	100	60	588(±74)	59(±7)
5[d]	**1**	1000	60	60	186(±14)	19(±1)
6[d]	**1**	1000	80	30	620(±36)	62(±4)
7[d]	**1**	1000	80	10	398(±14)	40(±1)
8[e]	**1**	10000	80	60	83(±27)	1(±0)
9[d,f]	**1**	3000	80	60	723(±40)	24(±1)
10[g]	**2**	1000	80	60	762(±105)	76(±11)
11[g]	**2**	1000	100	60	555(±15)	55(±1)
12[g]	**2**	1000	60	60	161(±6)	16(±1)
13[g]	**2**	1000	80	30	766(±81)	71(±14)
14[h]	**2**	10000	80	60	1229(±18)	12(±0)

[a] General reaction conditions: catalyst precursor (0.01 mmol); NaHCO$_3$ (10 mmol); MeOH (20 mL); H$_2$ pressure, 24 h. [b] Catalyst precursor **i**: 1 mL of a 0.01M stock solution of commercial P4 and Fe(BF$_4$)$_2$·6H$_2$O (1:1). [c] Catalyst precursor **1"**: 1 mL of a 0.01M stock solution of **1"** in PC. [d] Catalyst precursor **1**: 1 mL of a 0.01M stock solution of **1** in PC. [e] 0.1 mL of a 0.01M stock solution of **1** in PC. [f] 30.0 mmol NaHCO$_3$. [g] Complex **2** (0.01 mmol) was added to the autoclave from a CH$_3$CN stock solution, from which the solvent was subsequently removed (0.02 M, 0.5 mL, see Experimental Section for details). [h] Complex **2** (0.001 mmol) was added to the autoclave from a CH$_3$CN stock solution, from which the solvent was subsequently removed (0.02 M, 50 µL). [i] TON = mmoles of sodium formate per mmoles of catalyst. [j] Yields calculated from the integration of ^{1}H NMR signals due to NaHCO$_2$, using THF as internal standard. [k] Values of yields and TONs were calculated as

averages from the analysis of 2-4 samples, the largest deviations are reported in brackets; selected experiments were repeated to ensure reproducibility.

Formic Acid Dehydrogenation. FA dehydrogenation to H_2/CO_2 gas mixtures was tested in the presence of the *in situ* and pre-formed catalysts described above, using an inert solvent (PC) under isobaric conditions (1 atm) and in absence of added base, measuring the development of gas during the reaction with a manual gas-burette. The gas mixtures were analyzed off-line by FT-IR spectroscopy, showing absence of CO for all tests (detection limit 0.02%).[25] Much to our surprise, the well-defined catalyst precursor **2** (0.1 %mol) resulted inactive in the dehydrogenation of FA in PC at 40 °C. Thus, we targeted the use of *in situ* catalysts formed using *rac*- and *meso*-P4. Initially, we checked the activity of commercial P4 (0.1 %mol, *meso*/*rac* = ca. 3) under the same conditions described above, and observed a FA conversion of 4 % after 6 h, corresponding to a TON = 444 (Table 2; entry 1). When pure *rac*-P4 was used, generating *in situ* catalyst **1** (0.1 %mol) FA dehydrogenation proceeded with good conversions, reaching TON = 604 after 8 h at 40 °C (entry 2). As reported for the $PP_3/Fe(BF_4)_2{\cdot}6H_2O$ catalyst system,[5e] higher ligand/Fe ratios are beneficial to reach high reaction turnovers. Using a Fe/*rac*-P4 = 1/2 ratio,[5e] as expected the catalyst performance improved significantly, affording full conversion of FA in ca. 6 h (TON = 1000; entry 3). Using a catalyst/substrate ratio = 1:10000 at 40 °C, low conversions (11 %) were obtained after 6 h, with TON = 1081 (entry 5). Using the same catalyst/substrate ratio at 60 °C, gave a higher TON = 3088 after 6 h (entry 6). Using a higher Fe /ligand = 1:4 ratio, at 60 °C considerably enhanced catalytic activity was achieved (TON = 6061, 6h; entry 9). In contrast, pre-catalysts obtained from $Fe(BF_4)_2{\cdot}6H_2O$ and *meso*-P4 showed worse catalytic activities (generally ca. 33% lower) compared to *rac*-P4 (entries 4, 7,8 and 10). Selected results are summarized in Table 2. Selected reaction profiles (volumes *vs.* time) of catalytic runs obtained at catalyst/substrate = 1:10000 ratio, at various Fe/ligand ratios and temperatures, are shown in Figure 5. Disappointingly, recycling experiments at catalyst / substrate = 1:1000, Fe/ligand = 1:2, 40 °C showed a severe drop in activity from the first to the third cycle, namely from TON = 1000 to 295 after 6 h.

Mechanistic studies. The reactivity of the different pre-catalysts with FA was studied by monitoring stoichiometric reactions by NMR and by HPNMR *in operando* conditions. A solution of complex **2** (0.7 mL, 0.012 M in PC, C_6D_6 insert) was reacted with FA (1 equiv) for 1h in a NMR tube. No changes in the $^{31}P\{^1H\}$ and ^1H NMR spectra were observed even after heating to 60 °C, confirming that **2** is not reactive under these conditions, probably due to stable coordination of MeCN ligands to the Fe center.

In contrast, addition of 1 equivalent of FA to a solution of **1** in PC in a NMR tube (0.7 mL, 0.042 M, C_6D_6 insert) at room temperature, resulted in the formation of the monohydride [FeH(*rac*-P4)](BF_4) (**3**·BF_4) and of the formate complex [Fe(η^2-O_2CH)(*rac*-P4)](BF_4) (**6**.BF_4, δ_P 107.6 (t), 76.0 (t); $^2J_{PP}$ = 29.0, 28.9 Hz), initially in 6:1 ratio. Heating to 40 °C for 1h then leaving the tube overnight at 25 °C gave almost complete conversion to **3**·BF_4. The experiment was repeated in the presence of a large excess of FA (100 equiv) monitoring catalyst evolution by HPNMR spectroscopy. A 10 mm HPNMR sapphire tube was thus charged with a solution of **1** in PC (1.8 mL; 0.012 M), to which CD_3OD (0.4 mL) was added for deuterium lock.

Upon addition of FA at RT, complexes **3**·BF_4 and **6**·BF_4 were observed to form in 1:6 ratio. The probehead was then heated to 40 °C. After 1h, the reaction mixture evolved further with formation of a new species (**9**), characterized by four structured signals in the $^{31}P\{^1H\}$ NMR (see Experimental Section) and by a complex high field resonance signal (ddd; δ_H -9.55 ppm, $^2J_{PP}$ = 25.5, 46.5, 70.7 Hz; 1H, Fe*H*) in the corresponding ^1H NMR spectrum, indicative of the formation of an octahedral [FeHL(*rac*-P4)] complex with *cis*-α configuration. Prolonged heating resulted in the complete conversion to **9**, affording a yellow solution. Further multinuclear NMR analysis and ESI-MS spectroscopy data obtained from aliquots of the final solution allowed to identify complex **9** as the Fe-carbonyl hydrido complex *cis*-α-[FeH(CO)(*rac*-P4)](BF_4) (L = CO; for details see Experimental Section).[26]

As CO may result from the a competitive FA decomposition pathway, *i.e.* dehydration to H_2O and CO, we thought of interest to investigate further the reaction of **1** with FA. Some hints were given from the experimental data described above. Firstly, CO was never detected in the gas mixtures resulting from the catalytic runs by off-line FTIR measurements (see SI for a representative spectrum).[25] Secondly, complex **9** was never obtained in the NMR experiment carried out using a FA:**1** = 1:1 ratio. Thirdly, **9** was formed under isochoric conditions (HPNMR) in the presence of 100 equiv. of FA. Under these conditions, it is likely that the CO_2 pressure built up in the HPNMR tube during the course of the experiment may have undergone partial reductive disproportionation to CO and CO_3^{2-} as previously observed upon prolonged reaction of the monohydride **3**·BPh_4 with CO_2.

To confirm this hypothesis, we repeated the experiment in the glass reactor (isobaric conditions) normally used for the catalytic runs. Under the same conditions applied for the HPNMR experiment, gas evolution was complete after 20 min and again no CO was detected in the gas mixture. Furthermore, the mixture color remained purple throughout the run, whereas a bright yellow color should be expected upon formation of **9** in high concentrations. As further confirmation, NMR analysis of the catalytic mixture at the end of the run showed the typical $^{31}P\{^1H\}$NMR resonances of **3**·BF_4 and **6**·BF_4 in 1:1 ratio, while the signals due to **9** were not observed. Based on these data, although we cannot rule out that at low catalyst concentrations (0.01 %mol) catalyst deactivation may occur by formation of **9**, we propose that in closed (isochoric) vessels Fe-catalyzed CO_2 reductive disproportionation becomes a competing pathway, and CO coordination to **3**·BF_4 gives the stable (and catalytically inactive) octahedral **9**.

The following pathway for the base-free FA catalytic dehydrogenation reaction is thus proposed (Scheme 6). In step (i), the catalyst precursor **1**, formed *in situ* from $Fe(BF_4)_2{\cdot}6H_2O$ and *rac*-P4, reacts with FA to give the formate complex [Fe(η^2-O_2CH)(*rac*-P4)](BF_4) (**6**.BF_4), which after $\eta^2 \rightarrow \eta^1$ coordination shift from **6** to **6'** (ii) and rearrangement (iii), undergoes β-hydride elimination to give back **3**·BF_4 and CO_2 (iv). Protonation of **3**·BF_4 by FA results in the fast elimination of H_2 and regeneration of the formate complex **6**·BF_4 (v).

Table 2. Formic Acid Dehydrogenation catalyzed using *in situ* Fe(II) pre-catalysts.

Entry	Ligand	Sub-strate/cata-lyst	Fe/Ligand	T (°C)	V_{1h} (mL)[d]	TON_{1h}[e]	V_{final} (mL)[d]	TON_{final}[e]	Total Conv. (%)
1[a]	P4[c]	10000	1:2	40	25	97	115	444 (6h)	4
2[a]	*rac*-P4	1000	1:1	40	220	85	1560	604 (8h)	60
3[a]	*rac*-P4	1000	1:2	40	345	133	2570	1000 (6h)	100
4[a]	meso-P4	1000	1:2	40	165	64	810	313 (8h)	31
5[b]	*rac*-P4	10000	1:2	40	45	174	280	1081 (6h)	11
6[b]	*rac*-P4	10000	1:2	60	215	830	800	3088 (6h)	31
7[b]	meso-P4	10000	1:2	40	15	58	90	348 (6h)	3
8[b]	meso-P4	10000	1:2	60	70	270	260	1003 (6h)	10
9[b]	*rac*-P4	10000	1:4	60	400	1544	1570	6061 (6h)	61
10[b]	meso-P4	10000	1:4	60	140	540	590	2278 (8h)	23

Reaction conditions: [a] $Fe(BF_4)_2{\cdot}6H_2O$, 5.3 mmol; ligand (1 to 4 equiv. to Fe); HCOOH, 5.3 mol (2 mL); PC, 5 mL. [b] As above, $Fe(BF_4)_2{\cdot}6H_2O$, 5.3 µmol. [c] Commercial tetraphos-1 (P4) ligand, *meso*-P4/*rac*-P4 = 3. [d] Gas evolution measured by manual gas burette, based on 2-4 tests, error ± 10%. Gas mixture analyzed off-line by FTIR spectroscopy. [e] Defined as $mmol_{gas\ produced}$ / $mmol_{catalyst}$.

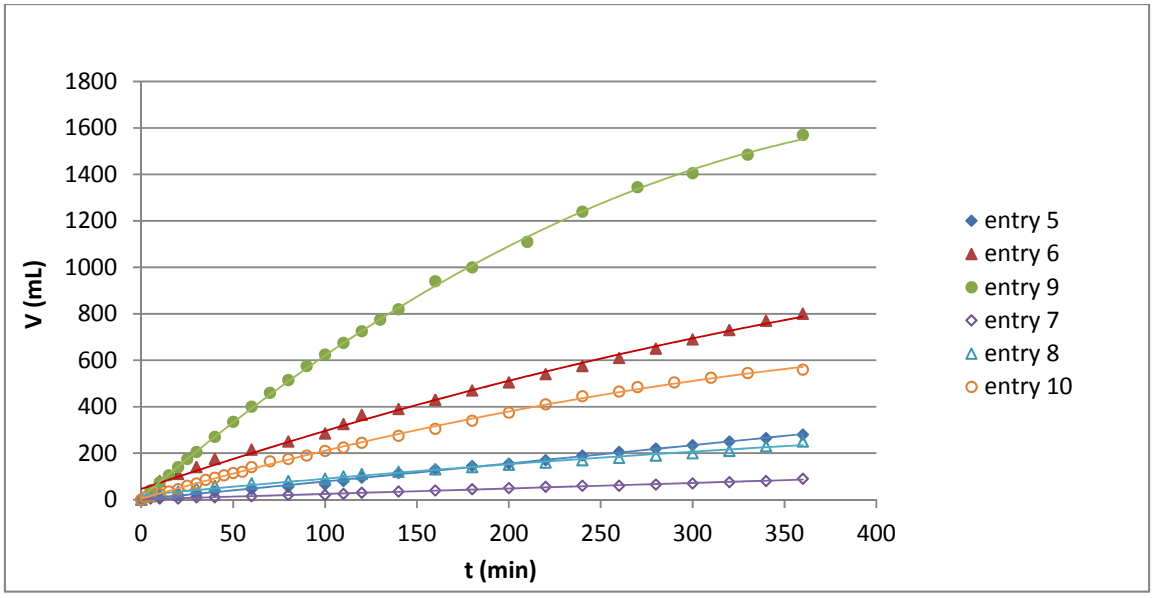

Figure 5. Reaction profiles of selected FA dehydrogenation catalytic runs using catalyst/substrate = 1:10000 ratio at different temperatures and Fe:P4 ratios. For legenda and conditions see Table 2.

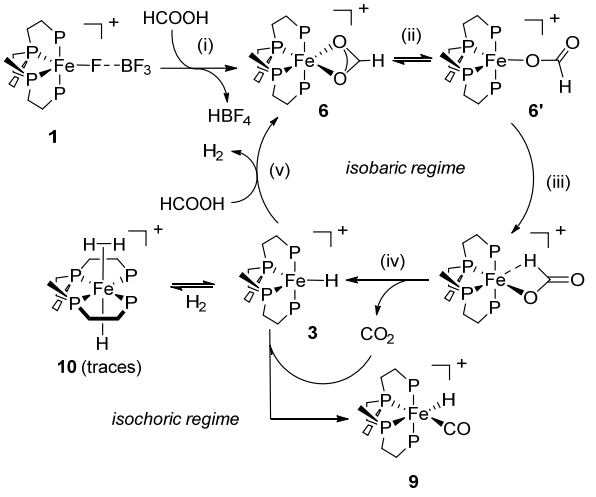

Scheme 6. Proposed mechanism for the catalytic dehydrogenation of FA.

CONCLUSIONS

In summary, the coordination chemistry of the *rac*- and *meso*-isomers of the linear tetraphosphine 1,1,4,7,10,10-hexaphenyl-1,4,7,10-tetraphosphadecane (tetraphos-1, P4) towards Fe(II) was explored in details, obtaining novel complexes which were applied as catalysts for base-free H_2/CO_2 generation from formic acid and for the hydrogenation of sodium bicarbonate to formate under mild conditions, showing a higher activity in the case of Fe/*rac*-P4 systems. Mechanistic studies highlighted the pivotal role of the monohydride $[FeH(rac\text{-P4})]^+$ in both reactions, and that CO_2 reductive disproportionation should not be underestimated as a competing pathway in the case of Fe(II)/polyphosphine systems. A full DFT study of both catalytic reactions promoted by Fe/tetraphos-1 is currently under way.

EXPERIMENTAL SECTION

GENERAL METHODS AND MATERIALS

All synthesis were performed using standard Schlenk techniques under an atmosphere of dry nitrogen or argon. Solvents were freshly distilled over appropriate drying agents, collected over Linde type 3A or 4A molecular sieves under nitrogen, and degassed with nitrogen or argon gas. Ligand 1,1,4,7,10,10-hexaphenyl-1,4,7,10-tetraphosphadecane (tetraphos-1, P4) was supplied by Pressure Chemicals Inc., Pittsburgh, PA. $[Fe(MeCN)_6](BF_4)_2$ was synthesized according to literature methods.[17] Anhydrous $FeCl_2$, $Fe(BF_4)_2{\cdot}6H_2O$ and propylene carbonate (PC) were purchased from commercial suppliers and used without further purification.

SYNTHETIC PROCEDURES.

Reaction of *rac*-P4 with $Fe(BF_4)_2{\cdot}6H_2O$. Ligand *rac*-P4 (67 mg, 0.1 mmol) was dissolved in propylene carbonate (PC) (2.0 mL) under gentle heating (40-50 °C) to afford complete dissolution. One equivalent of $Fe(BF_4)_2{\cdot}6H_2O$ (34 mg, 0.1 mmol) was added to the colorless solution, which immediately turned deep purple. $^{31}P\{^1H\}$ NMR analysis showed quantitative formation of a single product. The purple product could be precipitated by adding a large amount of Et_2O (at least 8.0 mL). The decanted solid was recovered by removing the colorless solution via cannula, and washed with Et_2O to remove all propylene carbonate yielding analytically pure complex $[Fe(\eta^1\text{-}FBF_3)(rac\text{-P4})](BF_4)$ (**1**). Due to the poor stability of **1** as isolated solid, we chose to use stock solutions of **1** in PC for both catalytic and NMR experiments. Yield: 78 mg (94%). $^{31}P\{^1H\}$ NMR (121.49 MHz, PC + C_6D_6 capillary): δ_P 99.9 (br.s.; 2P, *P*Ph), 60.9 ppm (br.s.; 2P, *P*Ph_2). $^{19}F\{^1H\}$ NMR (376.15 MHz, PC + C_6D_6 insert): δ_P 154 ppm (s.; 4F, B*F*$_4$)

Reaction of *meso*-P4 with $Fe(BF_4)_2{\cdot}6H_2O$. In a 5 mm NMR tube, *rac*-P4 (20 mg, 0.03 mmol) was dissolved in propylene carbonate (PC, 0.7 mL). Gentle heating (40-50 °C) was needed to afford complete dissolution of the ligand. One equivalent of $Fe(BF_4)_2{\cdot}6H_2O$ (10 mg, 0.03 mmol) was added to the colorless solution, which immediately turned brown and then yellow. $^{31}P\{^1H\}$ NMR analysis showed formation of $[Fe(\eta^1\text{-}FBF_3)(meso\text{-P4})](BF_4)$ (**1"**) as a single product. No attempts were made to isolate the product. $^{31}P\{^1H\}$ NMR (121.49 MHz, PC + C_6D_6 insert): δ_P 104.3 (br.s.; 2P, *P*Ph), 70.3 ppm (br.s.; 2P, *P*Ph_2).

Synthesis of *cis*-α-$[Fe(MeCN)_2(rac\text{-P4})](BF_4)_2$ (2). Ligand *rac*-P4 (134 mg, 0.2 mmol) was suspended in MeCN (10.0 mL) and the mixture was vigorously stirred until the tetraphosphine turned into a thin powder. One equivalent of $[Fe(MeCN)_6](BF_4)_2$ (95 mg, 0.2 mmol) was added to the white suspension, affording a bright orange solution. The reaction mixture was allowed to stir until a clear solution was obtained, and was subsequently stirred one more hour. The solution was then concentrated under vacuum to remove all volatiles. The resulting orange solid was then dissolved in a minimum volume of acetonitrile (ca. 0.5 mL). Addition of pentane resulted in the precipitation of analytically pure **2** as a crystalline, orange solid. Yield: 170 mg (87%). Crystals of **2** suitable for X-ray diffraction data collection were grown by adding pentane (4.0 mL) to an acetonitrile/methanol solution (0.5 + 1.0 mL) of **2**. $^{31}P\{^1H\}$ NMR (121.49 MHz, CD_3CN): δ_P 100.7 (t, $^2J_{PP}$ = 31.7 Hz; 2P, *P*Ph), 65.6 ppm (t, $^2J_{PP}$ = 31.7 Hz; 2P, *P*Ph_2). ESI-MS: calcd. for $^{12}C_{46}{}^1H_{48}{}^{14}N_2{}^{56}Fe^{31}P_4$, $[M]^+$: m/z = 404.10532, found: m/z = 404.10474.

Reaction of *meso*-P4 with $[Fe(MeCN)_6](BF_4)_2$. In an NMR-scale experiment, *meso*-P4 (13 mg, 0.02 mmol) was placed into an NMR tube, to which 0.5 mL of CD_3CN were added. The NMR tube was shaken vigorously to help dissolution of the ligand and subsequently $[Fe(MeCN)_6](BF_4)_2$ (ca. 10 mg, 0.02 mmol) was added, resulting in immediate color change to red-orange. The reaction mixture was analyzed by $^{31}P\{^1H\}$ NMR, which showed the formation of *trans*-$[Fe(MeCN)_2(meso\text{-P4})](BF_4)_2$ (*trans*-**2**) and *cis*-β-$[Fe(MeCN)_2(meso\text{-P4})](BF_4)_2$ (*cis*-β-**2**) in approximately 2:1 ratio. $^{31}P\{^1H\}$ NMR for *trans*-**2**: (121.49 MHz, CD_3CN): δ_P 85.4 (m; 2P, *P*Ph), 75.4 (m; 2P, *P*Ph_2). $^{31}P\{^1H\}$ NMR for *cis*-β-**2** (121.49 MHz, CD_3CN): δ_P 115.2 (m; 1P), 111.4 (m; 1P), 72.1 (m; 1P), 59.9 (m; 1P).

Synthesis of [FeH(*rac*-P4)](BPh$_4$) (3·BPh$_4$). In a flame-dried Schlenk tube kept under argon, *rac*-P4 (67 mg, 0.1 mmol) was dissolved in 3.0 mL of THF. A stoichiometric amount of anhydrous $FeCl_2$ (13 mg, 0.1 mmol) was added as a solid, and the resulting deep blue solution was allowed to stir for 5 min. at room temperature. $NaBPh_4$ (35 mg; 0.01 mmol) and MeOH (1.5 mL) were added to the reaction mixture, which was then stirred vigorously for about 10 min. $NaBH_4$ (4 mg, 0.1 mmol) was then added to the reaction mixture as a solid, and a vigorous reaction took place, affording an intense red mixture. All volatiles were removed under vacuum and the solid residue was re-dissolved in THF (8.0 mL). The resulting suspension was filtered via cannula into a second Schlenk tube kept under argon, affording a limpid red solution, from which all volatiles were removed under vacuum, affording analytically pure **3**·BPh$_4$. Yield: 114 mg (100%). Crystals suitable for X-ray diffraction data collection were obtained by adding MeOH to a THF solution of **3**·BPh$_4$. $^{31}P\{^1H\}$ NMR (*d*$_8$-THF, 121.49 MHz): δ_P 119.4 (t, $^2J_{PP}$ = 24.5 Hz; 2P, *P*Ph), 99.4 (t, $^2J_{PP}$ = 24.5 Hz; 2P, *P*Ph$_2$). ^1H NMR (*d*$_8$-THF, 300.13 MHz, negative region): δ_H -9.16 (t, $^2J_{HP}$ = 24.0 Hz; 1H, Fe*H*).

Synthesis of *cis*-α-[Fe(H)$_2$(*rac*-P4)] (4). The synthetic procedure described for the synthesis of *trans*-[Fe(H)$_2$(*meso*-P4)] was adapted with slight modifications.[14] A three-necked round bottom flask, equipped with reflux condenser was charged under argon with *rac*-P4 (67 mg, 0.1 mmol) and dry THF (2.5 mL). A solution of anhydrous $FeCl_2$ (13 mg, 0.1 mmol) in THF (2.5 mL) was added via cannula and the resulting mixture was allowed to stir for 10 min. $NaBH_4$ (20 mg, 0.55 mmol) was added as a solid, and the dark blue reaction mixture obtained was heated to reflux. As no visible changes occurred, additional THF (3.0 mL) was added, followed by another aliquot of $NaBH_4$ (10 mg, 0.27 mmol) and absolute EtOH (0.5 mL). As EtOH was added, a vigorous reaction took place and the deep blue mixture turned orange. After gas evolution had ceased, additional $NaBH_4$ (10 mg, 0.27 mmol) and absolute EtOH (0.5 mL) were added, and again, gas evolution was observed. The orange mixture was refluxed for about 10 min after gas evolution had ceased, after which it was allowed to cool to room temperature and filtered via cannula. The volume of the solution was partly reduced under vacuum and dry methanol was subsequently layered on top of the orange solution, from which bright yellow crystals formed. Yield: 53 mg (72 %). $^{31}P\{^1H\}$ NMR (*d*$_8$-THF, 121.49 MHz): δ_P 123.8 (t, $^2J_{PP}$ = 13.5 Hz; 2P, *P*Ph), 113.1 (t, $^2J_{PP}$ = 13.5; 2P, *P*Ph$_2$). ^1H NMR (*d*$_8$-THF, 300.13 MHz, negative region): δ_H -11.7 (m; 2H, Fe(*H*)$_2$). ESI-MS: calcd. for $^{12}C_{42}{}^1H_{43}{}^{56}Fe^{31}P_4$, $[M\text{-}H]^+$: m/z = 727.16592, found: m/z = 727.16523.

Reaction of 3·BPh$_4$ with CO$_2$. A few crystals of **3**·BPh$_4$ (ca. 10 mg) were placed in an NMR tube under argon and dissolved in *d*$_8$-THF (0.5 mL). CO_2 (1 atm) was then bubbled through the solution, whose color turned light purple. NMR analysis revealed quantitative formation of the expected formate complex [Fe(η^2-OCHO)(*rac*-P4)](BPh$_4$) (**6**·BPh$_4$). $^{31}P\{^1H\}$ NMR for **6**·BPh$_4$ (*d*$_8$-THF, 161.99 MHz): δ_P 106.0 (t, $^2J_{PP}$ = 28.5 Hz; 2P, *P*Ph), 76.5 (t, $^2J_{PP}$ = 26.1 Hz; 2P, *P*Ph$_2$). $^{13}C\{^1H\}$ NMR for **6**·BPh$_4$ (*d*$_8$-THF, 100.6 MHz): δ_C 162.4 (dd; $^2J_{PP}$ = 49.4 Hz, $^2J_{PP}$ = 98.7 Hz, BPh4), 171.9 [br. s., Fe(O$_2$*C*H)].

After 24h acquisition, the $^{31}P\{^1H\}$ NMR spectrum revealed the formation of carbonate complex [Fe(η^2-O$_2$CO)(*rac*-P4)] (**7**). Based on $^{31}P\{^1H\}$ NMR integration, complexes **5** and **7** resulted in approximately 1:0.6 ratio. $^{31}P\{^1H\}$ NMR for **7** (*d*$_8$-THF, 161.99 MHz): δ_P 104.7 (t, $^2J_{PP}$ = 30.4 Hz; 2P, *P*Ph), 71.3 (t, $^2J_{PP}$ = 30.4 Hz; 2P, *P*Ph$_2$). No $^{13}C\{^1H\}$ NMR resonance was observed for the carbonate O$_2$*C*O carbon atom of **7**.

Few purple crystals suitable for X-ray diffraction data collection were obtained by layering MeOH on top of the *d*$_8$-THF solution and standing for 1 day. The X-ray crystal structure revealed the serendipitous formation of trimetallic complex {μ^2-[Fe(MeOH)$_4$]-κ^1-*O*-[Fe(η^2-O$_2$CO)(*rac*-P4)]$_2$}(BPh$_4$)$_2$ (**7'**).

Reaction of 1 with K$_2$CO$_3$. 0.5 mL of a 0.01 M stock solution of **1** in PC were placed in a 5 mm NMR tube under argon. Solid K_2CO_3 (7.0 mg, 0.05 mmol) was then added. The solution in the NMR tube was stirred with a small stirring bar and the purple solution turned initially bright pink and then bright red. *d*$_8$-toluene (0.2 mL) was added for deuterium lock and the red solution was analyzed by $^{31}P\{^1H\}$ NMR and $^{13}C\{^1H\}$ NMR. $^{31}P\{^1H\}$ NMR analysis revealed the quantitative formation of carbonate complex **7**, whereas no $^{13}C\{^1H\}$ NMR resonance was observed for the carboxylic O$_2$*C*O carbon of **7**. $^{31}P\{^1H\}$ NMR for **7** (PC + *d*$_8$-toluene, 121.49 MHz): δ_P 104.7 (t, $^2J_{PP}$ = 30.4 Hz; 2P, *P*Ph), 71.3 (t, $^2J_{PP}$ = 30.4 Hz; 2P, *P*Ph$_2$).

Synthesis of *cis*-α-[FeH(CO)(*rac*-P4)](BF$_4$) (9). A 10 mm HPNMR sapphire tube was charged with a solution of Fe(BF$_4$)$_2$·6H$_2$O (14 mg; 0.04 mmol) and *rac*-P4 (28 mg; 0.04 mmol) in propylene carbonate (1.8 mL) under argon. CD_3OD (0.4 mL) was then added for deuterium lock, followed by HCOOH (0.15 mL, 4.15 mmol; 100 equiv. to Fe). The tube was closed and placed in the NMR probe. The probehead was gradually heated to 60 °C and the reaction was monitored by $^{31}P\{^1H\}$ NMR (see Supporting Information). The tube was left at 60 °C overnight, resulting in a yellow solution. $^{31}P\{^1H\}$ and ^1H NMR analysis revealed the quantitative formation of *cis*-α-[Fe(H)(CO)(*rac*-P4)](BF$_4$) (**9**). $^{31}P\{^1H\}$ NMR (121.49 MHz, CD_3OD): δ 114.6 (dt, $^2J_{PP}$ = 23.5, $^2J_{PP}$ = 38.6, 1P), 105.1 (br.dd., $^2J_{PP}$ = 8.6, $^2J_{PP}$ = 21.9; 1P), 100.9 (ddd, $^2J_{PP}$ = 10.5, $^2J_{PP}$ = 39.3, $^2J_{PP}$ = 68.7; 1P), 92.3 (dd, $^2J_{PP}$ = 37.9, $^2J_{PP}$ = 68.5; 1P). ^1H NMR (300.13 MHz, CD_3OD, negative region): δ -9.6 (ddd, $^2J_{PP}$ = 25.5, $^2J_{PP}$ = 46.5, $^2J_{PP}$ = 70.7; 1H, Fe*H*). $^{13}C\{^1H\}$ NMR (75.47 MHz, CD_3OD, carbonyl region): δ 162.77 (s; *C*O). A sharp singlet of higher intensity was also observed at δ 162.1 ppm for H*C*OOH. ESI-MS: calcd. for $^{12}C_{43}{}^1H_{43}{}^{56}Fe^{16}O^{31}P_4$ $[M]^+$: m/z =753.16550, found: m/z = 753.16517.

CATALYTIC TESTS

Catalytic sodium bicarbonate hydrogenation tests. In a typical experiment, a 40 mL magnetically stirred stainless steel autoclave built at CNR-ICCOM is charged under inert atmosphere (glovebox) with $NaHCO_3$ (typically 840 mg, 10 mmol) and the catalyst (0.01–0.001 mmol as solid or stock solution in PC). The autoclave is then closed and thoroughly purged through several vacuum/argon cycles. MeOH (20.0 mL) is then

added to the autoclave by suction. Finally the autoclave is pressurized with H_2 gas at the desired pressure. The autoclave is then placed into an oil bath pre-heated to the desired temperature and left stirring for the set reaction time. After the run, the autoclave is cooled in an ice/water bath, de-pressurized, and the catalytic mixture is transferred to a flask and concentrated under vacuum at room temperature. The formate content is determined by analyzing aliquots (ca. 30 mg) of the solid mixture dissolved in D_2O (0.5 mL) by ^1H NMR, using dry THF (20 μL) as internal standard with a relaxation delay of 20 seconds.

Catalytic formic acid dehydrogenation tests. In a typical experiment, a solution of catalyst (typically 5.3 mmol) in propylene carbonate (5 mL) is placed under an argon atmosphere in a magnetically stirred glass reaction vessel thermostated by external liquid circulation and connected to a reflux condenser and gas-burette (2 mL scale). After heating to 40-60 °C, HCOOH (2.0 mL) is added and the experiment started. The gas evolution is monitored throughout the experiment by reading the values reached on the burettes. The gas mixture is analyzed off-line by FTIR spectroscopy using a 10 cm gas-phase cell (KBr windows) to check for CO formation (detection limit 0.02%).

ASSOCIATED CONTENT

Supporting Information. General methods and equipment. NMR spectra and details of HPNMR experiments. Supplementary information on FA dehydrogenation tests. Cif files for X-ray crystal structures of **2**, **3**.BPh_4, **4**, **5** and **7'**. This material is available free of charge via the Internet at http://pubs.acs.org.

AUTHOR INFORMATION

Corresponding Authors

* l.gonsalvi@iccom.cnr.it

Author Contributions

All authors have given approval to the final version of the manuscript.

ACKNOWLEDGMENT

Financial contributions by CNR, MIUR and ECRF through projects EFOR, Progetto Premiale 2012 "Integrated and eco-sustainable technologies for the production, storage and use of the energy" and Firenze Hydrolab[2], respectively, are gratefully acknowledged. This work was also supported by COST Action CM1205 CARISMA (Catalytic Routines for Small Molecule Activation).

Table of Contents artwork

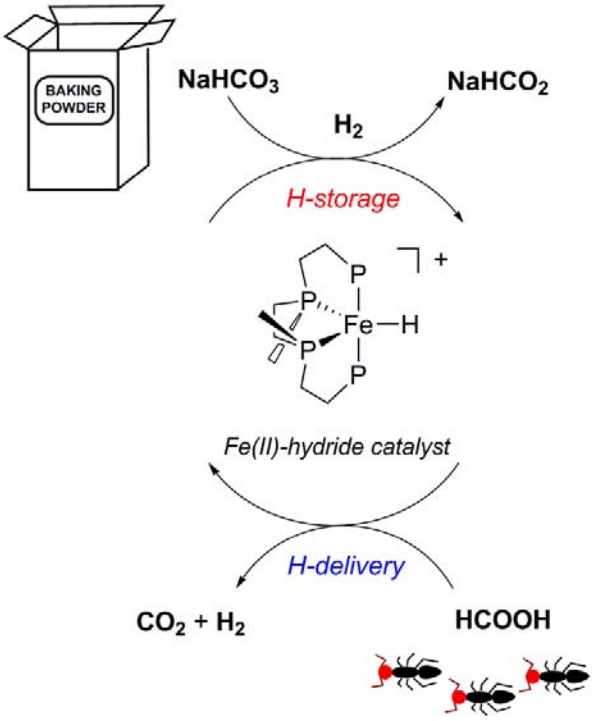

REFERENCES

(1) (a) Turner, J. A. *Science* **2004**, *305*, 972–974; (b) Schlapbach, L.; Züttel, A. *Nature* **2001**, *414*, 353–358; (c) Armaroli, N.; Balzani, V. *Angew. Chem. Int. Ed.* **2007**, *46*, 52–66; (d) Lubitz, W. *Chem. Rev.* **2007**, *107*, 3900–3903.

(2) (a) Joó, F. *ChemSusChem* **2008**, *1*, 805–808; (b) Enthaler, S. *ChemSusChem* **2008**, *1*, 801–804; (c) Federsel, C.; Jackstell, R.; Beller, M. *Angew. Chem. Int. Ed.* **2010**, *49*, 6254–6257; (d) Loges, B.; Boddien, A.; Gärtner, F.; Junge, H.; Beller, M. *Top. Catal.* **2010**, *53*, 902–914; (e) Enthaler, S.; Langermann, J.; Schmidt, T. *Energy Environ. Sci.* **2010**, *3*, 1207–1217.

(3) (a) Loges, B.; Boddien, A.; Junge, H.; Beller, M. *Angew. Chem. Int. Ed.* **2008**, *47*, 3962–3965; (b) Boddien, A.; Loges, B.; Junge, H.; Beller, M. *ChemSusChem* **2008**, *1*, 751–758; (c) Boddien, A.; Loges, B.; Junge, H.; Gärtner, F.; Noyes, J. R.; Beller, M. *Adv. Synth. Catal.* **2009**, *351*, 2517–2520; (d) Junge, H.; Boddien, A.; Capitta, F.; Loges, B.; Noyes, J. R.; Gladiali, S.; Beller, M., *Tetrahedron Lett.* **2009**, *50*, 1603–1606; (e) Boddien, A.; Gärtner, F.; Federsel, C.; Sponholz, P.; Mellmann, D.; Jackstell, R.; Junge, H.; Beller M. *Angew. Chem. Int. Ed.* **2011**, *50*, 6411–6414; (f) Boddien, A.; Federsel, C.; Sponholz, P.; Mellmann, D.; Jackstell, R.; Junge, H.; Laurenczy, G.; Beller, M. *Energy Environ. Sci.* **2012**, 8907–8911; (g) Huff, C. A.; Sanford, M. S. *ACS Catal.* **2013**, *3*, 2412–2416.

(4) (a) Tanaka, R.; Yamashita, R.; Nozaki, K. *J. Am. Chem. Soc.* **2009**, *131*, 14168–14169; (b) Hull, J. F.; Himeda, Y.; Wang, W. H.; Hashiguchi, B.; Periana, R.; Szalda, D. J.; Fujita, E., *Nature Chem.* **2010**, *4*, 383–388.

(5) (a) Federsel, C.; Boddien, A.; Jackstell, R.; Jennerjahn, R.; Dyson, P. J.; Scopelliti, R.; Laurenczy, G.; Beller, M. *Angew. Chem. Int. Ed.* **2010**, *49*, 9777–9780; (b) Boddien, A.; Gärtner, F.; Jackstell, R.; Junge, H.; Spannenberg, A.; Baumann, W.; Ludwig, R.; Beller, M. *Angew. Chem. Int. Ed.* **2010**, *49*, 8993–8996; (c) Boddien, A.; Loges, B.; Gärtner, F.; Toborg, C.; Fumino, K.; Junge, H.; Ludwig, R.; Beller, M. *J. Am. Chem. Soc.* **2010**, *132*, 8924–8934; (d) Langer, R.; Diskin-Posner, Y.; Leitus, G.; Shimon, L. J. W.; Ben-David, Y.; Milstein, D., *Angew. Chem. Int. Ed.* **2011**, *50*, 9948–9952; (e) Boddien, A.; Mellmann, D.; Gärtner, F.; Jackstell, R.; Junge, H.; Dyson, P. J.; Laurenczy, G.;

Ludwig, R.; Beller, M. *Science* **2011**, *333*, 1733–1736; (f) Ziebart, C.; Federsel, C.; Anbarasan, P.; Jackstell, R.; Baumann, W.; Spannenberg, A.; Beller, M. *J. Am. Chem. Soc.* **2012**, *134*, 20701–20704; (g) Sánchez-de-Armas, R.; Xue, L.; Ahlquist, M. S. G. *Chem. Eur. J.* **2013**, *19*, 11869–11873; (h) Yang, X. *Dalton Trans*. **2013**, *42*, 11987–11991.

(6) (a) Federsel, C.; Ziebart, C.; Jackstell, R.; Baumann, W.; Beller, M. *Chem. Eur. J.* **2012**, *18*, 72–75; (b) Jeletic, M. S.; Mock, M. T.; Appel, A. M.; Linehan, J. C. *J. Am. Chem. Soc.* **2013**, *135*, 11533–11536.

(7) The iron catalyzed decomposition of formic acid by [FeH(η^2-H_2)(PP_3)]BPh_4 was briefly reported in earlier literature, see: Bianchini, C.; Peruzzini, M.; Polo, A.; Vacca, A.; Zanobini, F. *Gazz. Chim. It.* **1991**, 121, 543 – 549. Another highly active Fe-pincer based system, however needing Lewis acids and higher temperatures (80 °C) to reach TON of ca. 10^6, was reported very recently, see: Bielinski, E. A.; Lagaditis, P. O.; Zhang, Y.; Mercado, B. Q.; Würtele, C.; Bernskoetter, W. H.; Hazari, N.; Schneider, S. *J. Am. Chem. Soc.* **2014**, *136*, 10234–10237.

(8) These hydrides were originally described by: Bianchini, C.; Laschi, F.; Peruzzini, M.; Ottaviani, M. F.; Vacca, A.; Zanello, P. *Inorg. Chem.* **1990**, *29*, 3394-3402.

(9) (a) Mellone, I.; Peruzzini, M.; Rosi, L.; Mellmann, D.; Junge, H.; Beller, M.; Gonsalvi, L. *Dalton Trans.* **2013**, *42*, 2495–2501; (b) Manca, G.; Mellone, I.; Bertini, F.; Peruzzini, M.; Rosi, L.; Mellmann, D.; Junge, H.; Beller, M.; Ienco, A.; Gonsalvi, L. *Organometallics* **2013**, *32*, 7053–7064; (c) Bosquain, S. S.; Dorcier, A.; Dyson, P. J.; Erlandsson, M.; Gonsalvi, L.; Laurenczy, G.; Peruzzini, M. *Appl. Organomet. Chem.* **2007**, *21*, 947–951;

(10) Erlandsson, M.; Landaeta, V. R.; Gonsalvi, L.; Peruzzini, M.; Phillips, A. D.; Dyson, P. J.; Laurenczy, G. *Eur. J. Inorg. Chem.* **2008**, *4*, 620–627.

(11) Brown, J. M.; Canning, L. R. *J. Organomet. Chem.* **1984**, *267*, 179–190.

(12) Bautista, M. T.; Earl, K. A.; Maltby, P. A.; Morris, R. H.; Schweitzer, C. T. *Can. J. Chem.* **1994**, *72*, 547–560.

(13) King, R. B.; Heckley, P. R.; Cloyd, J. C. Jr.; *Z. Naturforsch B.* **1974**, *296*, 574–575.

(14) Bautista, M. T.; Earl, K. A.; Maltby, P. A.; Morris, R. H. *J. Am. Chem. Soc.* **1988**, *110*, 4056–4057.

(15) King, R. B.; Kapoor, P. N. *J. Am. Chem. Soc.* **1969**, *91*, 5191–5192.

(16) (a) King. R. B.; Kapoor. R. N.; Saran. M. S.; Kapoor. P. N. *Inorg. Chem.* **1971**, *10*, 1851–1860; (b) King, R. B.; Kapoor, P. N. *J. Am. Chem. Soc.* **1971**, *93*, 4112–4119, 4158–4166; (c) Ghilardi, C. A.; Midollini, S.; Stoppioni, P.; Sacconi, L. *Inorg. Chem*. **1973**, *12*, 1801–1805; (d) Bacci, M.; Ghilardi, C. A., *Inorg. Chem.* **1974**, *13*, 2398–2403; (e) Ghilardi, C. A.; Midollini, S.; Sacconi, L.; Stoppioni, P. *J. Organomet. Chem*. **1981**, *205*, 193–202; (f) Bacci, M.; Ghilardi, C. A.; Orlandini, A. *Inorg. Chem* **1984**, *23*, 2798–2802; (g) Brown, J. M.; Canning, L. R. *J. Organomet. Chem.* **1984**, *267*, 179–190; (h) Rivera, V. A.; De Gil, E. R.; Fontal, B. *Inorg. Chim. Acta* **1985**, *98*, 153–159; (i) Brüggeller, P. *Inorg. Chem.* **1990**, *29*, 1742–1750; (j) Goller, H.; Brüggeller, P. *Inorg. Chim. Acta*, **1992**, *197*, 75–81; (k) Chen, J.-D.; Cotton, F. A.; Hong, B. *Inorg. Chem*. **1993**, *32*, 2343–2353; (l) Cotton, F. A.; Hang, B.; Shang, M.; Stanley, G. G. *Inorg. Chem.* **1993**, *32,* 3620–3627; (m) Chen, J.-D.; Cotton, F. A.; Hong, B. *Inorg. Chem.* **1993**, *32*, 2343–2353; (n) Jia, G.; Lough, A. J.; Morris, R. H. *J. Organomet. Chem.* **1993***, 461,* 147–156; (o) Dillinger, K.; Oberhauser ,W.; Bachmann, C.; Brüggeller, P. *Inorg. Chim. Acta* **1994**, *223*, 13–20; (p) Airey, A. L.; Swiegers, G. F.; Willis, A. C.; Wild, S. B. *J. Chem. Soc., Chem. Commun.* **1995**, 693–694; (q) Oberhauser, W.; Bachmann, C.; Brüggeller, P. *Polyhedron* **1995***, 14*, 787–792; (r) Oberhauser, W.; Bachmann, C.; Brüggeller, P. *Polyhedron* **1996**, *15*, 2223–2230.

(17) (a) Hathaway, B. J.; Holah, D. G.; Underhill, A. E. *J. Chem. Soc.* **1962**, 2444–2448; (b) Heintz, R. A.; Smith, J. A.; Szalav, P. S, Weisgerber, A.; Dunbar, K. R. *Inorg. Synth.* **2004**, *33*, 75–78.

(18) Beck, W.; Sünkel, K. *Chem. Rev.* **1988**, *88*, 1405–1421.

(19) Habeck, C. M.; Hoberg, C.; Peters, G.; Näther, C.; Tuczek, F. *Organometallics* **2004**, *23*, 3252–3258.

(20) (a) Kubas, G. J. "Heterolytic Splitting of HH, Si-H, and Other s Bonds on Electrophilic Metal Centers." *Adv. Inorg. Chem.* **2004**, *56*, 127–178; (b) Schlaf, M.; Lough, A. J.; Maltby, P. A.; Morris, R. H. *Organometallics* **1996**, *15*, 2270–2278.

(21) Field, D. L.; Lawrence, E. T.; Shaw, W. J.; Turner, P. *Inorg. Chem.* **2000**, *39*, 5632–5638.

(22) (a) Allen, O. R.; Dalgarno, S. J.; Field, L. D. *Organometallics* **2008**, *27*, 3328–3330; (b) Allen, O. R.; Dalgarno, S. J.; Field, L. D.; Jensen, P.; Willis, A. D. *Organometallics* **2008**, *27*, 2092–2098.

(23) For other examples on the reductive disproportionation of CO_2 catalyzed by iron complexes, see: (a) Antberg, M.; Frosin, K.-M.; Dahlenburg, L. *J. Organomet. Chem.* **1988**, *338*, 319–327; (b) Sadique, A. R.; Brennessel, W. W.; Holland, P. L. *Inorg. Chem.* **2008**, *47*, 784–786.

(24) As the $^{31}P\{^1H\}$ AA'XX' pattern of **8** does not allow to discriminate between Oh and TBP geometries, we tentatively propose that the corresponding signals may be due to the formation of either *cis*-α-[Fe(η^1-$O_2COH)_2$(rac-P4)] or *cis*-α-[Fe(η^1-$O_2CO)_2$(rac-P4)].

(25) Gas mixtures analyses were carried out by FTIR spectroscopic method described by Wills et al. For details see: (a) Morris, D. J.; Clarkson, G. J.; Wills, M. *Organometallics* **2009**, *28*, 4133-4140; (b) Guerriero, A.; Bricout, H.; Sordakis, K.; Peruzzini, M.; Monflier, E. Hapiot, F.; Laurenczy, G.; Gonsalvi, L. *ACS Catal.* **2014**, *4*, 3002-3012.

(26) Another species, characterized by $^{31}P\{^1H\}$ signals at 130.3 and 89.6 ppm was observed to form in traces after heating the solution to 40 °C (under 1 bar H_2) or 60 °C (HPNMR experiment). Based on literature data concerning the *meso*-P4 analogue,[14] we tentatively assign these resonances to *trans*-[FeH(η^2-H_2)(*rac*-P4)]$^+$ (**10**). Notably, the relative concentration of **10** did not seem to change significantly throughout the rest of the experiment.